A model for calculating the erosion distance of soft sea cliff under wave loading

CHANG Fangqiang[1]*, SHU Zhonglei[1]

[1] Faculty of Civil Engineering, Huaqiao University, Xiamen 361021, China

Abstract

A model for calculating the erosion distance of soft sea cliff under wave loading is established based on the erosion mechanism of soft sea cliff under wave loading and for considering wave hydrodynamic and sea cliff material parameters. The model is verified, and the parameters are regressed using an indoor flume experiment. The erosion distances of the sea cliff in the northeast of the Pingtan Island are calculated by the model, and the results are compared with the measured data. The maximum erosion occurs in static water level, the location of the maximum erosion moves up as the wave continues, and the erosion stops when the wave lasts for a period of time. The erosion does not occur until the wave height exceeds a critical value; however, the contribution of large waves to the erosion is not relatively substantial. The calculated erosion distances at two places in the northeast of Pingtan Island are 0.32 m and 0.26 m.

Key words: wave, soft sea cliff, erosion

---

1 Introduction

Sea cliffs suffer severe erosion and retreat worldwide, particularly on the east coast of England, the Baltic, the southern North Sea, north of Lake Great Britain, the west coast of Cape Cod, California and the Denglou Cape, southwest of the Leizhou Peninsula of China; the maximum retreat rate is approximately 1–2 m/a (Sunamura, 1992; Lee, 1997; Lee et al., 2001; Wang et al., 2002). Severe erosion also occurs in the provinces of Zhejiang, Fujian, Guangdong, Zhuang Autonomous Region of Guangxi, and Hainan in China and leads to gradual decrease in land areas. Retreat is a threat to the security of local engineering facilities; sea cliff erosion intensifies with annual increase in global warming and sea levels, thereby prompting the local government to build breakwaters or other protective measures (Trenhaile, 2010). Understanding sea cliff erosion rates and its position in the following years are important for implementation of protective sea cliffs and land use planning. In engineering design lifetime, sea cliff erosion should not be a threat to the engineering security on the top of the cliff. Moreover, determining the protection time is necessary for facilities facing threats of erosion.

Most theoretical works, including studies on an erosion rate and an erosion distance, have focused on erosion and retreat because of severe erosion of sea cliffs. The increase in sea level promotes cliff erosion. Bray and Hooke (1997) proposed a semi-empirical method for calculating the retreat rate. Most predictive models of cliff recession focus on storm surges in conjunction with cliff profile changes; Fisher and Overton (1984) and Nishi and Kraus (1996) proposed models in which erosion from the impact of individual waves is used to determine the amount of erosion. The total amount of erosion can be determined using the frequency and intensity of wave impacts, multiplied by an empirical transport coefficient (Gelinas and Quigley, 1973; Mano and Suzuki, 1998; Erikson et al., 2007). Predictive models are used to calculate the retreat distance at few cliffs in the next hundreds or thousands of years (Trenhaile, 2009, 2010). A wave impact theory has been empirically validated and successfully employed to simulate cliff erosion in small and large wave flume studies and in the field (Fisher and Overton, 1984; Overton et al., 1994; Nishi and Kraus, 1996). However, developing an equation for predicting a transport coefficient has been rarely investigated. Although retreat modeling has focused on describing the gross features of cliff erosion, no attempt has been made to resolve the mechanism and to elucidate the details of the erosion process.

The mechanism and process of erosion of sea cliff under waves are analyzed in this paper. The development of governing equations and associated analytical solutions are described in the proceeding part. The eroded cliff material is not directly damaged by a wave pressure. The waves in front of the sea cliff produce the erosion force, which must be larger than the resisting force of the cliff material if erosion occurs. The eroded cliff material must overcome two types of force, namely, shear strength around the cliff material section and tensile strength behind the cliff material section. Analytical solutions are established based on erosion and resisting force theory.

A small-scale wave flume experiment is performed to elucidate the short-term time-evolution of sea cliff during erosion by using a series of waves. Three cliff models with different strengths in the flume are prepared for erosion. The erosion distance and time are recorded. The flume has two main purposes, namely, validating the erosion process of cliff eroded by waves and devel-

*Corresponding author, E-mail: malcme@126.com

oping the conversion coefficient in the predictive model based on the observed data. The model is then applied in the field, the erosion distances of the sea cliff on the northeast of the Pingtan Island are calculated, and the results are validated by data determined *in situ*.

2 Theoretical development

2.1 *Erosion mechanism of soft sea cliff*

Soft sea cliff generally comprises aeolian sand, residual soil, and eluvial loose gravel deposits, and the strength is relatively low compared with rock sea cliff. Therefore, soft sea cliff is likely to erode when strong waves attack, causing a severe retreat. Such problems usually occur when strong typhoons are encountered in coastal areas in the southeast of China. The role of the wave on the sea cliff face is very complex, which includes forces such as hydraulic pressures, tension, and shear stress. The wave causes great pressure when shallow water rushes on the cliff face, rotating the wave direction on the cliff face, which results in a eddy current and a eddy shear stress. Finally, vacuum suctions, which are called "reflux suctions" are formed when the wave goes back to the ocean, resulting in tension on the cliff face.

Cliff material is in a passive state of compression when the wave pressure acts on the cliff face. By contrast, cliff material is in a failure state when the wave pressure reaches the following values (Das, 1979):

$$p_0 = 2c\tan(45 + \varphi/2) + \sigma'\tan^2(45 + \varphi/2), \tag{1}$$

where σ' is the vertical effective stress, $\sigma' = \gamma z$, γ is the cliff material gravity, z is the cliff material depth; and c and φ are the cohesion and internal friction angle, respectively.

The value of Eq. (1) is usually above 100 kPa for the normally consolidated cliff material and the wave pressure on the cliff face is just tens of kilopascals; therefore, the cliff material would not be damaged and eroded under the wave pressure. Although the wave pressure is not a direct cause of sea cliff erosion, the wave pressure is a dynamic load which enables the sea cliff to soften or liquefy, thus leading to a reduction in a cliff material strength and an increase in cliff material erosion. Thus, the shear stress and the tension, which are two forces induced by a wave vortex, are the direct causes of the erosion on the cliff face. The establishment of an erosion model by considering the wave pressure and softening or liquefaction, shear stress and tension, as well as cliff material characteristics, is very difficult; therefore, the few conditions should be simplified.

Waves can only reach the cliff foot and the nearby upper position for homogeneous and tall sea cliffs; therefore, the erosion often occurs at the cliff foot and simultaneously forms sea notches (Trenhaile et al., 1998). The upper sea cliff loses support with the gradual development of sea notches. A large-scale slump could occur when the sliding force caused by gravity exceeds the stabilizing force (Hampton, 2002; Young and Ashford, 2008). In addition, the slump could cause a large-scale erosion once. Therefore, the erosion of the sea cliffs begins from the development of sea notches.

2.2 *Governing equations*

During the day of a typhoon, strong waves generated in deep-sea areas propagate landward; meanwhile, the wave energy is gradually attenuated and the wave height is reduced because of the friction between the bed surface and water points (Balsillie

and Tanner, 2000). As previously mentioned, sea cliff erosion is mainly caused by the shear stress and tension stress of waves; the two stresses are combined into one force, namely, the erosion force. The erosion force increases with the wave height and the wave pressure and can be expressed with wave pressure (Sunamura, 1977, 1982):

$$F_w = Ap, \tag{2}$$

where F_w is the erosion force; A is the conversion coefficient from the wave pressure to the erosion force; and p is the wave pressure.

The wave pressures on the cliff face and a breakwater are very similar; thus, the method for calculating the wave pressure on the breakwater is denoted. There are numerous methods to calculate the wave pressure, and the method of the shallow water wave pressure from Japan (The First Harbor Survey and Design Engineering Institute of Ministry of Transportation, 1994) is applied.

For shallow waters, the wave pressure can be expressed as

$$p = \rho g H \frac{\cosh k(d + z)}{\cosh kd}, \tag{3}$$

where ρ is the density of sea water; g is the gravity accelerate; H is the wave height in front of the sea cliff; k is a wave number, $k = 2\pi/L$, L is a wave length; d is the water depth in front of the sea cliff; and z is the water depth below the static surface. At $z = H$, the wave pressure $p = 0$; at the static water surface ($z = 0$), the wave pressure is at a maximum, $p_m = \rho g H$;

If cliff material erosion occurs, the erosion force must exceed the cliff material erosion resistance, that is $F_w \geqslant F_r$, in which F_r is the cliff material erosion resistance. If the portion of the cliff material separates from the cliff face because of erosion, the erosion body (separation body) must overcome two forces: the first is the anti-shear force surrounding the erosion body which is provided by the cliff material shear strength, and the second is the anti-tension force behind the erosion body which is provided by the cliff material tension strength, as shown in Fig. 1. One cell area of the erosion body was chosen for analysis, and then the anti-erosion force can be expressed as

$$F_r = 4d_e\tau + \sigma_t, \tag{4}$$

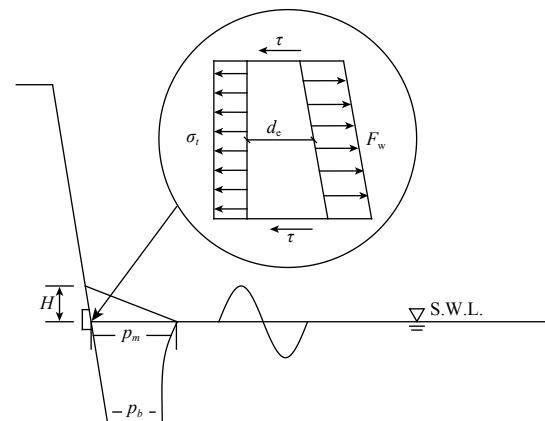where d_e is the erosion thickness of the sea cliff which is induced

Fig. 1. Forces on the erosion body on the cliff face.

by one wave; τ is the untrained shear strength; and σ_t is the tension strength, $\sigma_t = c \tan \phi$.

On the static water surface, the erosion occurs when Eq. (3) is equal with Eq. (4), further obtaining

$$d_e = \frac{A p_m - \sigma_t}{4\tau} = \frac{A \rho g H - \sigma_t}{4\tau}. \tag{5}$$

If erosion occurs, then coefficient A is

$$A = \sigma_t / p_m, \tag{6}$$

or

$$H_{crit} = \frac{\sigma_t}{\rho g A}, \tag{7}$$

where H_{crit} is the critical erosion wave height.

One wave period is treated as a unit of time; thereafter, the erosion rate can be expressed as the derivative of the distance X of the erosion time t,

$$\frac{dX}{dt} = \frac{A \rho g H - \sigma_t}{4\tau}. \tag{8}$$

When the wave lasts for a period of time Δt, the erosion distance is

$$X = \left(\frac{A \rho g H - \sigma_t}{4\tau} \right) \Delta t. \tag{9}$$

A certain range of the wave height has a certain frequency wave because the wave height usually follows a certain probability distribution, as shown in Fig. 2.

The erosion distance induced by wave group i (wave height H_i) is

$$X_i = \left(\frac{A \rho g H_i - \sigma_t}{4\tau} \right) \Delta t_i, \Delta t_i = \delta_i \Delta t, \tag{10}$$

where Δt_i is the duration of action of the wave group i; and δ_i is the occurrence frequency of the wave group i, $\delta_i = N_i / N$, N_i is the number of occurrence of the wave group i, and N is the total

Fig. 2. Schematic of frequency distribution occurrence of the wave height at the cliff base.

number of wave occurrences during the interval of Δt.

Based on Eq. (7), the erosion would not occur until the wave height exceeds the critical wave height. If $H_{crit} = H_j$, then the total erosion distance is

$$X = \sum_{i=j}^{n} X_i = \sum_{i=j}^{n} \left(\frac{A \rho g H_i - \sigma_t}{4\tau} \right) \delta_i \Delta t, \tag{11}$$

where X is the total erosion distance during a strong typhoon.

The conversion coefficient from the wave pressure to the erosion force A in Eq. (11) is unknown and would only be determined in the following flume experiment, wherein the calculation model would also be verified.

The wave parameters in front of the sea cliff are calculated based on the wave parameters in the deep-sea water because of insufficient wave observation settings in front of the sea cliff. The calculation method is shown in the Appendix.

3 Laboratory flume experiment

3.1 *Conditions of the experiment*

Three flume experiments are performed and the erosion distance with time is observed to show the erosion process of sea cliffs and verify the reasonability of the preceding established models. The flume size is 3 000 mm × 200 mm × 800 mm in length, width and height, with one wave-making plate driven by an electric motor in one end of the flume. The motor is made in Germany with ten frequency converters which can produce different wave heights and wave periods.

First, the sea cliff models in one end of the flume are fabricated. The model comprises granite residual cliff material obtained from the site in the northeast of the Pingtan Island using the process of crushing, drying, water mixing, and compaction. A rubber mallet was used to compact the cliff material with different times to create different intensities of the sea cliff model. Although the cliff material is compacted, its strength is much lower than *in situ* because the cliff material is remolded and the internal structure of the cliff material is destroyed, preventing its formation in a short period. The water content of the cliff models is controlled at approximately 30%, which is close to the values *in situ*. The height of the model is 60 cm and the slope angle is controlled between 85° and 88°. Sand beach was laid in front of the cliff face with a length 100 cm and a slope of 5° to simulate the effect of the beach on the erosion of sea cliff. In this study, three experiments are performed using different strengths of the cliff model. After completing the model, the undrained shear strength of each sea cliff model is tested by a portable vane shear instrument and the cliff material samples are withdrawn from the top of the cliff using a cutting ring to determine shear strength indexes such as cohesion and internal friction angle using a shear apparatus. A few 1 cm² square grids were drawn outside the wall of the flume to easily observe the morphological changes of the cliff model. After preparing the cliff model, the motor was started to make waves. When the cliff model obviously changes, its profiles are delineated with a brush on the sidewall of the flume. The cliff material properties of the cliff models and the hydrodynamic conditions in the experiment are shown in Table 1. The randomness of the waves is ignored because the waves in the flume are artificially made by a wave plate.

3.2 *Results of the experiment*

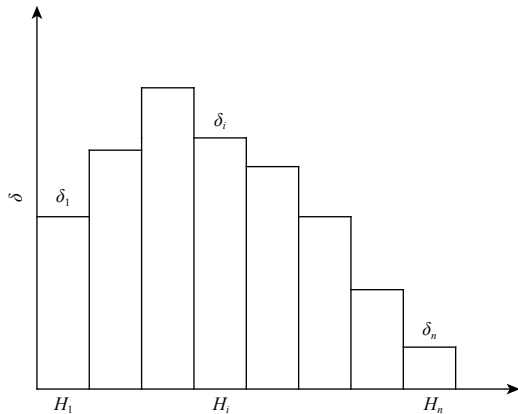The sea cliff profiles at different time are recorded during the

Table 1. Cliff material properties and dynamic water parameters in the flume test

| Conditions	Indexes	1	2	3
Cliff material properties	undrained shear strength/kPa	14.2	11.5	12.0
	cohesion/kPa	8	4	6
	internal friction angle/(°)	9	6	7
Hydrodynamics	water depth/cm	25	25	35
	wave height/cm	13	12	15
	period/s	5	5	5
	wave length/m	1.1	1.3	1.4

experiment, and their relationships in the three experiments are plotted in Fig. 3. (1) In each experiment, the sea cliff gradually retreats with the wave actions. In Experiment 1, the cliff reaches a steady state, that is, no erosion occurs with the waves when the wave erodes for 15 h. (2) In the early period of time, the maximum erosion occurred in the vicinity of the static water line because the wave pressure is the largest at the S.W.L. In Experiments 2 and 3, the maximum erosion moves upward with the wave actions because the strength of the cliff material is relatively low, thus resulting in the collapse of the upper cliff material of the notch. (3) The sea cliff eroded profiles are not smooth curves, which are caused by the nonuniformity of the cliff material in the cliff models. (4) The eroded lower boundary of the profiles is at the height of the wave trough; however, the upper boundary is higher than that of the peak height because of the continuous upper cliff material collapse with the wave. The lower boundary moves upward because most of the eroded cliff material accumulates at the foot of the cliffs, which weakens the wave energy and reduces the erosion. (5) In Experiments 2 and 3, the eroded profiles reach the surface of the flume glass and the overlying cliff material is in a complete suspension, preventing the collapse at the end of the experiment because of the low strength of the cliff material when the wave erodes for 8–9 h and because of the strong bonding force between the cliff material and the glass side of the flume.

In theory, the wave pressure is at the maximum at the S.W.L., and the maximum erosion should also occur at the S.W.L. if the collapse is ignored. The relationship between the erosion distance and time at the S.W.L. is shown in Fig. 4.

The basis of the data in Fig. 4, the conversion coefficient from the wave pressure to the erosion force A in the Eq. (9) is calculated. In Experiments 1–3, A lies between 1.11 and 1.34, 0.98 and 1.60, and 0.88 and 1.52, respectively. In Experiment 1, the cliff model compacted to a higher strength, and the strength of the cliff material is relatively uniform; therefore, the variance of coefficient A is small. However, in Experiments 2 and 3, coefficient A has larger variances.

4 Engineering application

The soft sea cliff is extensively distributed on the south coast of Fujian Province, from the Minjiang River Estuary to the south, including Fuqing and Pingtan, Putian, Quanzhou, Xiamen, and Zhangzhou, and the distribution length is approximately 320 km (Liu et al., 2010). The cliff height ranges from a few meters to tens of meters. These sea cliffs generally comprise granite weathering residual cliff material, old red sand, and aeolian sand, in which the two former cliff materials are compressed and over-consolidated for a long time; therefore, their strength is generally high. However, there are a number of strong typhoons each year in Fujian Province, causing large waves in the coastal area. These
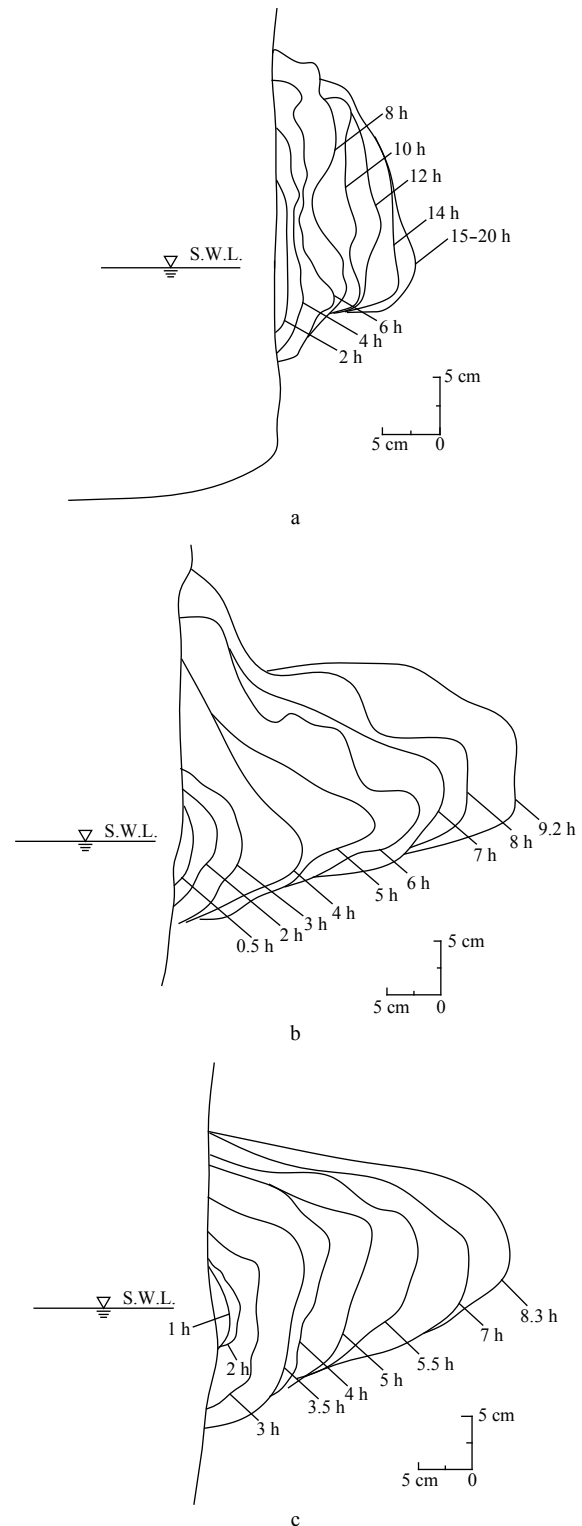
Fig. 3. Erosion distance of the cliff versus time in the flume test. Figures 3a, b and c are results of Experiments 1, 2 and 3, respectively.

waves result in the rapid erosion of sea cliffs, with an average annual erosion rate of approximately 1.87 m/a (Liu, 2010). One typical eroded soft sea cliff in the northeast of the Pingtan Island, which lies between the Liushui Wharf to the Shilou Village, is selected for calculation as shown in Fig. 5. This cliff has retreated landward by approximately 80 m in the past 40 a (Liu et al., 2010).
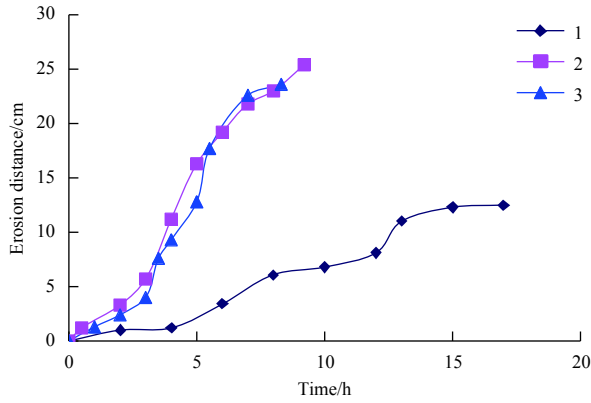
Fig. 4. Erosion distance versus time at the static water level.

The dominant and strong wave directions are NNE and NE, respectively. The tide is semidiurnal, with a maximum tidal range of 7.16 m and an average of 4.54 m (Liu et al., 2010; Cai et al., 1992). The field investigation finds that numerous slumps have accumulated at the foot of the cliff (Fig. 5). The slumps appear loose and a few are blocky. The sea cliff has been protected twice (the first was constructed in the 1990s and the second was being constructed from 2013) to prevent the continued erosion. The first protection is near the Shilou Village, which is approximately 600 m long. The lower component is a dry masonry stone retaining wall with a thickness of 0.7–1.6 m and a height of 1.3–2.5 m, and the upper component is a layer of stone. This protection has been severely damaged, which was induced by strong waves in the past 20 a. The failed stone scattered on the beach and has lost its protection. The second protection is a concrete breakwater with a length approximately 800 m, and its stiffness and strength is much greater than the first protection; however, the cost is relatively high.

The two profiles of the sea cliff in the study area are selected

for erosion calculation by the established theoretical method in this paper, namely, Profiles 1 and 2. The locations are shown in Fig. 5.

4.1 *Environmental conditions in the study area*

The environmental conditions related to the erosion calculation include hydrodynamic conditions caused by waves, sea cliff geometry and cliff material properties.

4.1.1 *Hydrodynamic conditions*

Several strong typhoon waves are induced by tropical storms at the study area, which resulted in severe cliff material erosion. On the basis of statistics, a total of 157 typhoons affected Pingtan from 1973 to 2008, with an average of four point five times per year (Liu, 2010). The typhoon mainly occurs from mid-May to mid-November period, particularly from July to September each year, thereby constituting approximately 70% of the total number.

On the basis of wave monitor statistics data within 21 a at Pingtan Marine Monitor Station (25°27′N, 119°51′E), the general maximum wave height H_{max} during a typhoon is 7.1–9.5 m, the average wave period T is 5.3–5.4 s (Compilation Committee of Chinese Bay, 1991), and the surge water depth can reach 2.0–3.0 m.

Different typhoon wind speeds and atmospheric pressures can produce different wave conditions. A few reprehensive wave conditions are generated based on wave statistics empirical formulations (Wen and Yu, 1984),

$$\left. \begin{array}{l} H_{max} = 2.663\bar{H} \\ H_{1/10} = 2.032\bar{H} \\ H_{1/3} = 1.598\bar{H} \end{array} \right\}, \tag{12}$$

$$\left. \begin{array}{l} T_{max} = 1.414\bar{T} \\ T_{1/10} \approx \bar{T} \\ T_{1/3} = 0.937T_{max} \end{array} \right\}. \tag{13}$$
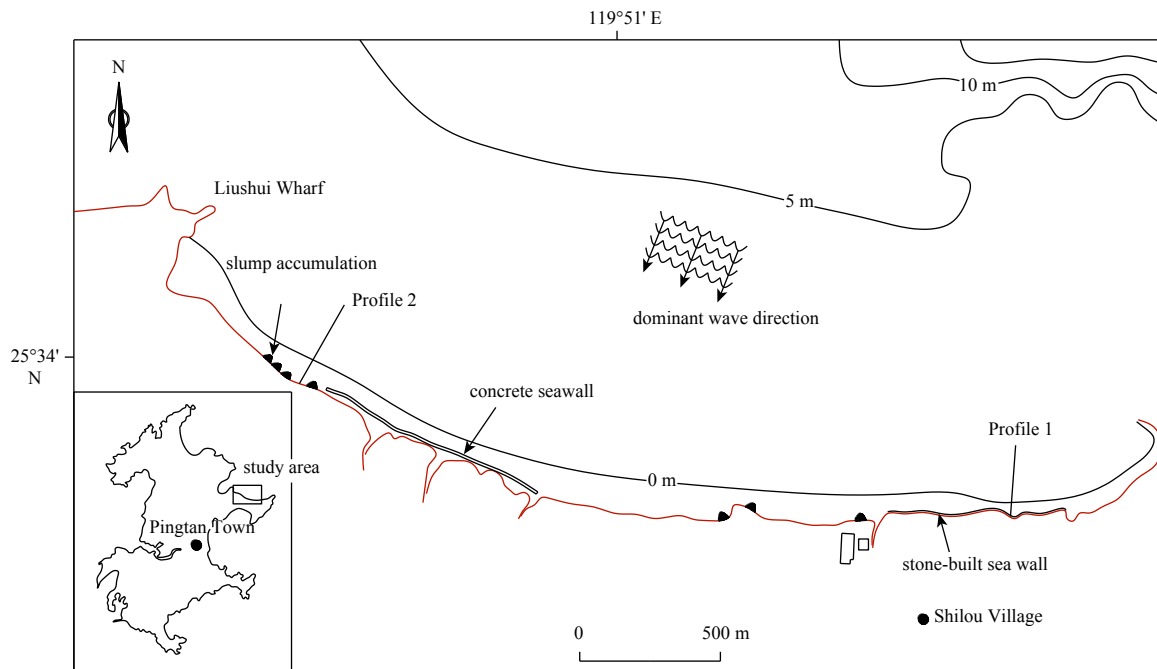

Fig. 5. Overview of the study area.

On the basis of Eqs (12) and (13), the average wave height $\overline{H}$ of the typhoon is approximately 2.7–3.6 m, with an average period $\overline{T}$ of 5.4 s. The wave parameters in the shallow water are calculated based on the data from the wave monitor station in the deep water because of insufficient wave monitor data in the shallow water in front of the sea cliff, which is in accordance with Appendix. The water depth at the monitor station is 53.0 m, the average wave height H_0 is 3.1 m, the wave direction angle is 45°, and the water depth in the shallow water is 2.5 m. The calculated wave parameters in the shallow water are shown in Table 2.

Table 2. Cliff geometry parameters, cliff material properties, and dynamic water parameters in the northeast of Pingtan Island

	Parameters	Profile 1	Profile 2
Geometry	cliff height/m	15.0	10.5
	slope angle/(°)	85.0	77.0
Cliff material	unit weight/kN·m⁻³	14.2	11.5
	fine particle content/%	62.0	57.0
	cohesion/kPa	58.4	54.2
	internal friction angle/(°)	25.6	32.8
	undrained shear strength/kPa	105	94.0
Hydrodynamic	water depth/m	2.5	2.5
	wave height/m	2.7	2.7
	wave period/s	5.4	5.4
	wave length/m	25.2	25.2

A few studies have shown that wave height and wave length fit the Rayleigh distribution (Notle and Hsu, 1972; Wen and Yu, 1984). Thus, a certain number of random waves in front of the sea cliff is generated based on its distribution, average wave height, and the lasting time of the strong waves and its period. Generally, a strong typhoon wave focusing at one area usually lasts for several hours to ten hours. For example, if the average wave height is 2.7 m, the wave period is 5.4 s and the duration of the strong wave is 8 h; thereafter, the number of random waves in front of the sea cliff is 5 333 (Fig. 6).

4.1.2 *Sea cliff geometries and cliff material properties*

The slopes of the sea cliff at the study area are quite steep, with an angle located between 60° and 88°. The cliff is mostly in a sunshine and windy environment; therefore, the water content, which is generally less than 35%, is low. The heights and slope angles of Profiles 1 and 2 at the study area are determined. Thereafter, the undrained shear strength of the cliff material is determined using portable vane shear apparatus, and cliff material samples are obtained from the foot of the cliff and transported to the laboratory to test its mechanical and physical properties. All the test methods are in accordance with the Chinese code "standard for soil test method" (GBT50123-1999). The main cliff material parameters are summarized in Table 2.

4.2 *Results and discussion*

The duration of the strong typhoon is obtained as 8 h, and the frequency δ_i and duration Δt_i of the wave height H_i are shown in Fig. 6, in which the duration of different heights is equal to the frequency multiplied by the total duration. On the basis of Eq. (11), the erosion of Profiles 1 and 2 in which the conversion coefficient from the wave pressure to the erosion force A uses the average values from the experiment, that is $A = 1.24$, is calculated. It
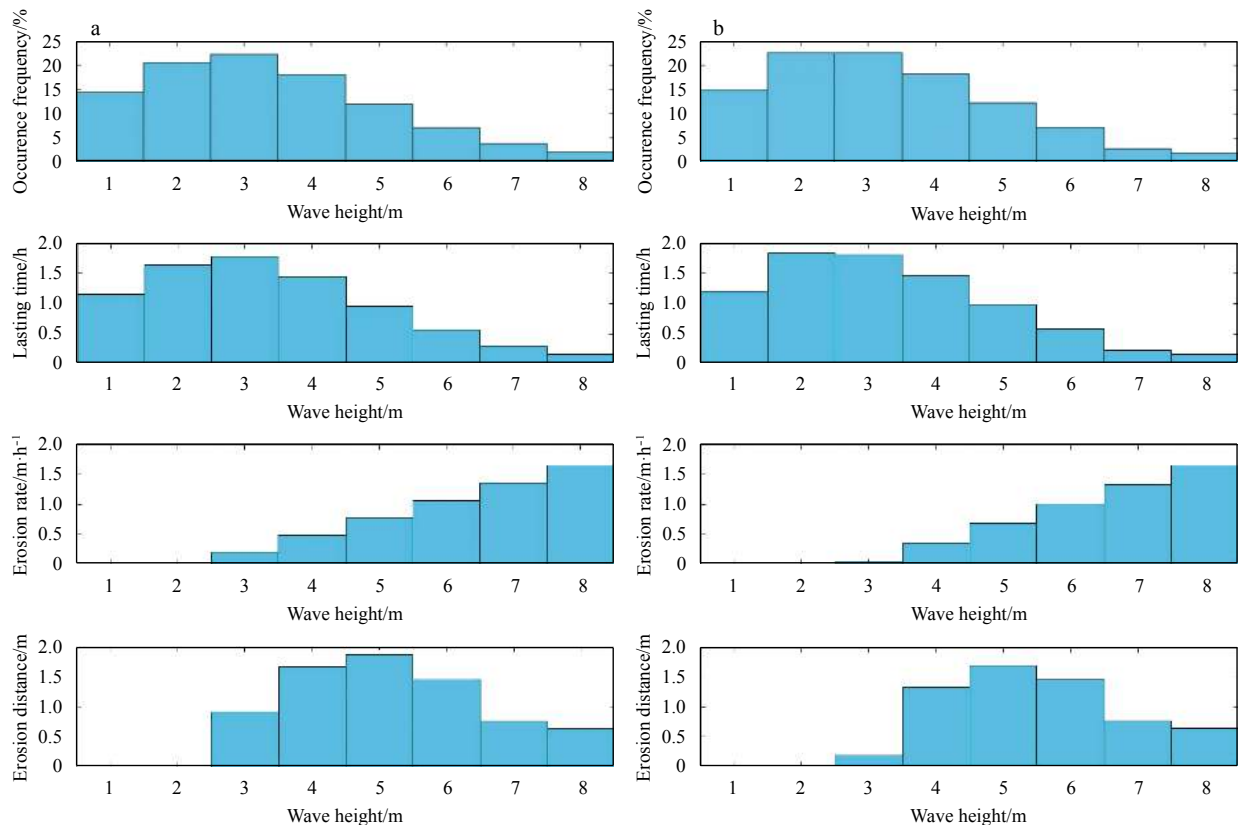

Fig. 6. Wave occurrence frequency, wave duration, erosion rate and recession distance versus cliff wave height. a. Pesult of Profile 1, and b. result of Proile 2.

is worth noting that the value of the conversion coefficient is obtained by flume test with small waves and low hardness in the paper. It is perhaps more accurate to reflect the value by observing the wave and erosion amount *in situ*, but this method is extremely difficult. Limited to the current test conditions, the flume test is maybe the only way to obtain the value of the conversion coefficient. In the flume test, the seek of the conversion coefficient has been considered the wave force and the strength of the cliff material, and the strength indexes include an undrained shear strength cohesion and an internal friction angle. The reliability to predict the actual soft sea cliff erosion using the conversion coefficient=1.24 need to be verified by more projects. The predicted results of the two sections using the conversion coefficient=1.24 in this paper are consistent with the measured results, but the applicability of other projects is to be further validated.

The calculated erosion rates dX/dt and the erosion distances X are also shown in [Fig. 6]. The diagram of the relationship between the wave height and the erosion rate shows that when the wave height is less than the critical value, the erosion rate is 0; that is, the wave height must exceed the critical value when erosion occurs. In these two profiles, the critical erosion wave heights H_{crit} are all 3.0 m, and the erosion rate increases with the wave height. The erosion distance X_i can be obtained by multiplying the erosion rate dX/dt with the corresponding duration Δt_i. Finally, all the erosion distances X_i are summed, the total erosion distance at Profiles 1 and 2 are goten, that are 0.31 and 0.25 m, respectively. The diagram of the relationship between the wave height and the erosion distance shows that only waves with larger height can produce significant erosion; conversely, small waves cannot cause erosion. However, the contribution to the erosion of larger waves is not substantially large because of its low frequency. Usually, the small waves can erode the slumping cliff material at the foot of the cliff because the slumping cliff material has been strongly disturbed and its strength is relatively low, making it easily erodible. The total erosion distance X is divided by the total duration Δt. The average erosion rates obtained are 0.038 8 and 0.031 3 m/h at Profiles 1 and 2, respectively.

The erosion distance and erosion rate at the study area are also determined and calculated by other methods. [Liu (2010)] calculated the erosion rate by using an average Rate method based on 50 a shoreline change and found that the average erosion rate is 1.25 m/a in 1961–1983 and 1.46 m/a in 1983–2009, which presented an increasing rate trend. The determined shoreline change of the three profiles from July 2007 to August 2008 is 1.32, 3.27, and 0.84 m, with an average of 1.81 m. The erosion distances of the two profiles are 0.31 and 0.25 m at each strong typhoon by the theoretical model in this paper; thereafter, the erosion distances are 1.40 and 1.13 m when multiplied by the average number of typhoons each year four point five times, which are close to the average determined *in situ*.

On the basis of Marine Forecast Station data of Fujian Province, the strong typhoons which affected the study area are relatively less in the past 3 a. The strong typhoons occurred twice in 2013 and 2014 and only once in 2015. The erosion distance in the last 3 a is relatively less based on the calculating methods in this paper.

5 Conclusions

A theoretical model for calculating the erosion of sea cliff under wave loading is established by analyzing wave loading, the cliff material properties of the sea cliff, and the mechanism of wave erosion. The model is validated and its parameter was regressed through the flume experiment. This model considered the wave intensity, the duration, and the cliff material engineering properties. Finally, the erosion rate and distance of sea cliffs in the northeast of Pingtan Island are calculated by this model. A few conclusions are as follows

(1) The flume test show that the maximum erosion first occurs near the static water level line and moves upward as waves continue, and the erosion would finally stop when the wave lasts for a certain period of time.

(2) The regression of results in the flume shows that the average value of coefficient A is 1.24.

(3) Cliff erosion would not occur until the wave height exceeds a critical value, in which the erosion rate is higher with the wave height; however, the contribution of larger waves to erosion is not considerably large because of its low frequency.

(4) The calculated erosion distances of the two cliffs in the northeast of Pingtan Island are 0.31 and 0.25 m under each strong typhoon acting for 8 h, and the annual erosion distances are 1.40 and 1.13 m if the number of typhoons is 4.5 a^{-1}, which are close to the values determined *in situ*.

References

Balsillie J H, Tanner W F. 2000. Red flags on the beach; part II. Journal of Coastal Research, 16(3): 3–5

Bray M J, Hooke J M. 1997. Prediction of soft-cliff retreat with accelerating sea-level rise. Journal of Coastal Research, 13(2): 453–467

Cai Aizhi, Gong Jinmei, Cai Yue'e. 1992. Transgression and eolian sand sequence in Luyuanpu Plain, Haitan Island, Fujian. Journal of Oceanography in Taiwan Strait, 11(2): 112–117

Compilation Committee of Chinese Bay. 1994. Chinese Bay, Volume VII (in Chinese). Beijing: China Ocean Press, 166–169

Das B M. 1979. Introduction to Soil Mechanics. Ames: The Iowa State University Press, 7–30

Eagleson P S, Dean R G. 1966. Small amplitude wave theory. In: Ippen A T, ed. Estuary and Coastline Hydrodynamics. New York: McGraw-Hill, 20–21

Erikson L H, Larson M, Hanson H. 2007. Laboratory investigation of beach scarp and dune recession due to notching and subsequent failure. Marine Geology, 245(1–4): 1–19

Fisher J S, Overton M F. 1984. Numerical model for dune erosion due to wave uprush. In: Proceedings of the 19th Coastal Engineering Conference. Houston: Coastal Engineering, 1553–1558

Gelinas P J, Quigley R M. 1973. The influence of geology on erosion rates along the north shore of Lake Erie. In: Wilson J B, Roff J, eds. Proceedings of the 16th Conference on Great Lakes Research. Minnesota: International Association Great Lakes Research. 421–430

Hampton M A. 2002. Gravitational failure of sea cliffs in weakly lithified sediment. Environmental & Engineering Geoscience, 8(3): 175–191

Lee E M. 1997. Landslide risk management: key issues from a British perspective. In: Cruden D M, Fell R, eds. Landslide Risk Assessment. Rotterdam: Balkema, 227–237

Lee E M, Hall J W, Meadowcroft I C. 2001. Coastal cliff recession: the use of probabilistic prediction methods. Geomorphology, 40(3–4): 253–269

Liu Jianhui. 2010. Analysis of mechanism and influencing factors of coastal erosion in Fujian Province (in Chinese)[dissertation]. Qingdao: Ocean University of China

Liu Jianhui, Cai Feng, Lei Gang, et al. 2010. Recession mechanic and process analysis of soft cliff on Fujian coast-In case of northeast coast of Pingtan Island. Marine Environmental Science (in Chinese), 29(4): 525–530

Mano A, Suzuki S. 1998. A dimensionless parameter describing sea cliff erosion. In: Proceedings of the 26th International Conference on Coastal Engineering. American Society of Civil Engineers, Copenhagen, American Society of Civil Engineers. 2520–

2533

Nishi R, Kraus N. 1996. Mechanism and calculation of sand dune erosion by storms. In: Proceedings of the 25th Coastal Engineering Conference. Orlando, Coastal Engineering, 3034–3047

Notle K G, Hsu F H. 1972. Statistics of Ocean Wave Groups. In: Offshore Technology Conference. Dellas, Texas. Offshore Technology Conference, 637–644

Overton M F, Pratikto W A, Lu J C, et al. 1994. Laboratory investigation of dune erosion as a function of sand grain size and dune density. Coastal Engineering, 23(1–2): 151–165

Sunamura T. 1977. A relationship between wave-induced cliff erosion and erosive force of waves. The Journal of Geology, 85(5): 613–618

Sunamura T. 1982. A predictive model for wave-induced cliff erosion, with application to Pacific coasts of Japan. The Journal of Geology, 90(2): 167–178

Sunamura T. 1992. The Geomorphology of Rocky Coasts. Chichester, UK: Wiley, 301–302

The First Harbor Survey and Design Engineering Institute of Ministry of Transportation. 1997. Port Engineering Design Manual (Middle Volume)(in Chinese). Beijing: People's Traffic Press, 31–41

Trenhaile A S. 2009. Modeling the erosion of cohesive clay coasts. Coastal Engineering, 56(1): 59–72

Trenhaile A S. 2010. Modeling cohesive clay coast evolution and response to climate change. Marine Geology, 277(1–4): 11–20

Trenhaile A S, Pepper D A, Trenhaile R W, et al. 1998. Stacks and notches at Hopewell Rocks, New Brunswick, Canada. Earth Surface Processes and Landforms, 23(11): 975–988

Wang Lirong, Zhao Huanting, Song Chaojing, et al. 2002. Coastal geomorphic evolution at the Denglou Cape, the Leizhou Peninsula. Acta Oceanologica Sinica, 21(4): 597–611

Wen Shengchang, Yu Zhouwen. 1984. Wave Theory and Calculation Principles (in Chinese). Beijing: Science and Technology Press, 177–195

Young A P, Ashford S A. 2008. Instability investigation of cantilevered seacliffs. Earth Surface Processes and Landforms, 33(11): 1661–1677

Appendix:

The wave height changes as it propagates from the deep-water zone to the shallow water zone because of the influence of the friction of seabed. The average wave height in the inshore zone (Seaport Hydrology Standard, JTS145-2-2013) can be calculated as following formulations:

$$H = H_0 K_s K_r, \tag{A1}$$

$$K_s = H/H_0' = \sqrt{L_0/(2nL)}, \tag{A2}$$

$$n = \frac{1}{2}\left(1 + \frac{2kd}{\sinh 2kd}\right). \tag{A3}$$

On the basis of Airy wave theory, the relationship between the wave length L and the water depth d (Eagleson and Dean, 1966) can be expressed as,

$$L = (g/2\pi)T^2 \tanh(2\pi d/L). \tag{A4}$$

If the bathymetric contours are parallel, the refractive coefficient can be expressed as

$$K_r = \sqrt{b_0/b} = \sqrt{\cos\alpha_0/\cos\alpha}. \tag{A5}$$

On the basis of Snell theory,

$$\sin\alpha = L/L_0 \sin\alpha_0. \tag{A6}$$

where K_s is the coefficient of shallow water; K_r is the refractive coefficient, H_0' is the calculated wave height in the deep water, L_0 and L are the wave lengths of the deep water and shallow water respectively, k is the wave number; d is the water depth in deep water; b_0 and b are the widths of the two adjacent wave rays in the deep water and the shallow water respectively; and α_0 and α are the wave angles in the deep water and the shallow water, respectively.